

SCIENTIFIC RESEARCH AND DEVELOPMENT

OXIDATION RESISTANCE OF NANO-REINFORCED PC-REFRACTORIES MODIFIED WITH PHENOL FORMALDEHYDE RESIN. PART 4. THERMODYNAMIC EVALUATION OF PHASE FORMATION WITHIN Mg–O–C–Al, Mg–O–C–Ni AND MgO–Al₂O₃–NiO–SiO₂ SYSTEMS USING SiC + Al + Ni (NiO) COMPLEX ANTIOXIDANT¹

G. D. Semchenko,^{2,6} O. N. Borisenko,³ D. A. Brazhnik,² S. M. Logvinkov,³
V. V. Povshuk,² I. Yu. Shuteeva,⁴ L. A. Angolenko,² N. S. Chopenko,⁵ and P. A. Vasyuk²

Translated from *Novye Ogneupory*, No. 7, pp. 23 – 33, July, 2017.

Original article submitted June 17, 2016.

Results are given for the synthesis and co-existence of phases formed from components of complex organic-inorganic antioxidant formed during modification of phenol-formaldehyde resin (PFR) and graphite with silica alkoxide and inorganic or organic nickel precursors. Thermodynamic analysis is given for the Mg–Al–C and Mg–O–Ni–C systems. It is shown that the periclase and carbon can coexist with aluminum and nickel, and also that oxidized antioxidants Al₂O₃ and NiO can interact respectively with the periclase and with the synthesized SiC formed during modification of PFR with silica. In considering the NiO–MgO–Al₂O₃–SiO₂ system it is established that during service noble spinel will be synthesized from the complex antioxidant components, facilitating an increase in PC-refractory durability in service.

Keywords: periclase-carbon (PC) refractories, phenol formaldehyde resin (PFR), organic-inorganic complex, complex antioxidant, thermodynamic analysis, Mg–Al–O–C, Mg–Ni–O–C and Ni–Mg–Al–Si systems.

It is normal to use Al as an antioxidant for MgO–C-refractories [1 – 3], whose greatest effect develops at above 1100°C; Metallic Si behaves similarly [4], although its use in the composition of PC-refractories is undesirable due to a significant reduction in refractoriness. During service aluminum metal is not only oxidized but it reacts with carbon with formation of aluminum carbide Al₄C₃ [5, 6]. Since Al and Al₄C₃ exhibit considerable affinity for oxygen, they are

readily oxidized with oxygen and slag iron oxides, which reduces carbon oxidation rate [7].

Oxidation products of aluminum metal in PC-refractories enter into chemical reaction fine periclase refractory binder and from spinel MgO·Al₂O₃ whose synthesis explains the increase in refractory corrosion resistance. However, with an Al concentration > 3% object disintegration is observed, connected with volumetric changes during MgO·Al₂O₃ synthesis not compensated by refractory porous structure [7] that limits the Al content in PC-refractory charges (used in charges up to 2%).

As antioxidants in producing PC-objects materials are used having high oxygen affinity underservice conditions compared with carbon [8, 9]; these are Al, Mg, and other metals, including Ni. The role of additive comes down not only to participation in processes reducing oxygen partial pressure, but also to participation in phase formation at a material surface, providing conditions for forming new struc-

¹ Parts 1 and 2 were published in *Novye Ogneupory* Nos. 9 and 11 (2016), and part 3 in No. 1 (2017).

² National Technical University, Kharkov Polytechnic Institute, Khar'kov, Ukraine.

³ Semen Kuznets Khar'kov National Economic University, Khar'kov, Ukraine.

⁴ Akvatika, Khar'kov, Ukraine.

⁵ Yu. Kondratyuk Poltava National technical University, Poltava, Ukraine.

⁶ galashabanova@ukr.net

tures with improved strength and corrosion characteristics. This method of stabilizing carbon is effective for the surface of objects in contact with molten metal or slag.

Currently another method is used for improving the oxidation resistance of carbon-containing magnesia refractories that includes a reduction in binder coking temperature (<1273 K) with formation of a crystalline graphite phase by adding a catalyst [10]. Catalysts are added in an amount of 0.1 to 10 wt.% of the weight of carbon binder. The catalysts used are readily reduced compounds of transition metals (Cu, Cr, Ni, Fe), and also metal catalysts of the type Ni, Pt, and Rh.

Considering this and also the high reaction activity of nickel ions with other compounds it is possible to consider use of nickel promising in preparing PC-materials, including nickel salts and a precursor of this antioxidant. In the presence of urotropine in PC-refractory charges during operation it is possible to reduce nickel salt [30]:



and nickel oxide formed already from precursor salt:



Presence of graphite in MgO–C-refractories facilitates an increase in their resistance to slag corrosion, to thermal shock, and a reduction in wettability and thermal expansion [11]. Undesirable changes in refractory properties occur with oxidation of graphite above 873 K. In order to protect graphite from oxidation within a refractory composition it is normal to add powder form antioxidants; in PC-refractories there is often use of aluminum proceeding from the condition that the metal exhibiting and greater tendency towards oxidation facilitates retention of a carbon phase [12]. However,

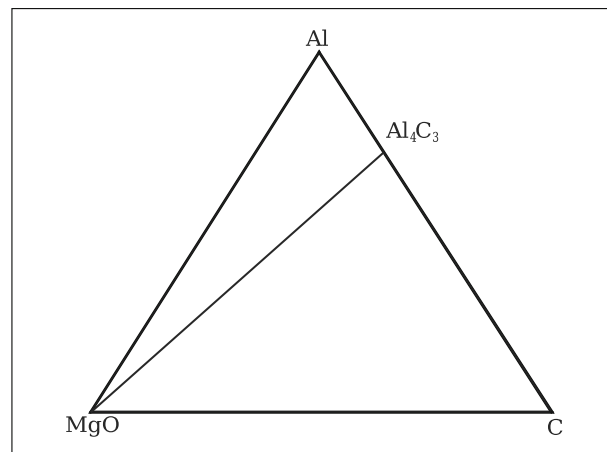


Fig. 1. MgO–C–Al system triangulation.

from results of numerous researches in the range 973 – 1873 K apart from Al_2O_3 formation of new phases is noted, such as Al_4C_3 and $\text{MgO} \cdot \text{Al}_2\text{O}_3$. The strength of PC-refractories with development of Al_4C_3 within their structure may increase, since its elasticity modulus by analogy with other metal carbides comprises 230 – 250 GPa [12].

More than a twofold increase in high-temperature ultimate strength in bending for PC-materials with use of Al antioxidant has been noted [13 – 15], which has been achieved due to forming Al_2O_3 and Al_4O_3 at high temperature (as intermediate phases) and $\text{Al}_4\text{O}_4\text{C}$ and Al_2OC according to known reactions of interaction of aluminum metal with CO, and also due to a reduction in open porosity of decarburized later as a result of the distribution of reaction products in pores with subsequent formation in objects of $\text{MgO} \cdot \text{Al}_2\text{O}_3$. In the Al–O–C system stable phases are Al, Al_4C_3 , Al_2O_3 , C, and also $\text{Al}_4\text{O}_4\text{C}$ and Al_2OC [16]. In the n Al–O–C system

TABLE 1. Substance Thermodynamic Constants

Substance	$-\Delta H_{f298}^0$, kJ/mole	ΔS_{298}^0 , J/(mole·K)	$C_p = a + bT + c'T^{-2}$			C_{p298}^0 , J/(mole·K)	Published source
			a , J/(mole·K)	$b \times 10^3$, J/(mole·K)	$c \times 10^{-5}$, J/(mole·K)		
MgO	601.53	27.42	42.62	7.28	–6.2	37.18	[20]
C _{gr}	—	5.69	17.17	4.27	–8.79	—	[20]
Al _c	—	28.365	20.68	12.39	—	24.37	[20]
MgAl ₂ O ₄	2314.9	80.68	154.07	26.79	–40.95	116.27	[20]
CO	110.51	198.0	28.43	4.10	–0.46	29.132	[20, 31]
CO ₂	393.69	213.82	44.17	9.04	–8.54	37.14	[20, 31]
Mg _c	—	32.53	22.32	10.26	–0.431	—	[20, 27]
Al ₄ C ₃	206.9	88.95	158.6	39.57	–28.64	116.779	[23]
α-Al ₂ O ₃	1676.8	50.95	114.84	12.81	–35.46	79.09	[21]
Al ₄ O ₄ C	2249.826	186.2	215.2	20.2	–64.0	—	[24]
Al ₂ OC	665.515	26.9	100.4	9.2	–29.7	—	[24]
Al ₃ O ₄	2145.042	59.5	153.8	22.0	—	—	[24]

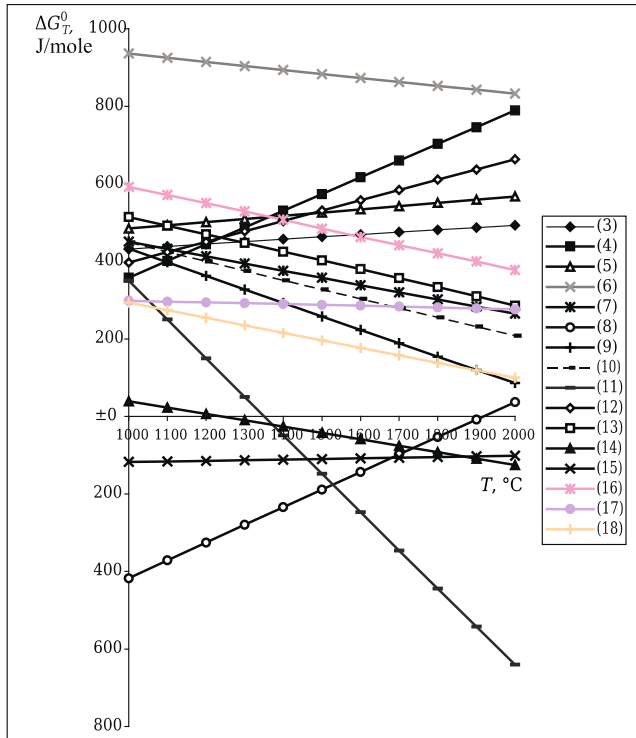


Fig. 2. Dependence of Gibbs energy ΔG_T^0 on temperature T for reactions (3) – (18) (see Table 2).

apart from oxycarbides presence has also been established by experiment of sub-oxides Al_2O and AlO [17], which in the presence of free carbon in a system form $\text{Al}_4\text{O}_4\text{C}$ and Al_2OC [18].

During operation of PC-refractories there is a reaction of carbothermal reduction of MgO [12, 25]. The reaction reaches equilibrium at 2123 K and with a reduction in pres-

sure (for example with use MgO-C -refractories in ladles in which there is metal for degassing) gaseous products of reaction of Mg and CO diffuse, and therefore the reaction continuous at lower temperature. In the Mg-C system formation has been established of MgC_2 and Mg_2C_3 carbides, although both carbides exist in a form of metastable phases, and a change in Gibbs energy with formation of these carbides from their components under standard conditions is favorable [19].

The aim of this research is to determine thermodynamic probability of forming phases from a mixture of periclase and organo-inorganic complexes in the range 1000 – 2000 K by studying the systems Mg-O-C-Al , Mg-O-C-Ni , and also reaction of phases formed during PC-refractory operation by studying the system $\text{MgO-Al}_2\text{O}_3\text{-NiO-SiO}_2$. First the authors considered the system MgO-C-Al . In view of the fact that this system contains one binary compound, i.e., Al_4C_3 , triangulation of the system MgO-C-Al has the form shown in Fig. 1. By predicting the possibility of formation (as a result of service to 1923 K) in materials of the system MgO-C-Al compounds $\text{MgO}\cdot\text{Al}_2\text{O}_3$, $\text{Al}_4\text{O}_4\text{C}$, Al_2OC , and Al_3O_4 , the authors decided to move too studying a four-component system Mg-O-C-Al . For a detailed study of this system three-component systems Mg-O-C , Al-O-C , Mg-O-Al , and Mg-C-Al were considered.

In order to establish the thermodynamic probability of coexistence of phase (for subsequent breakdown of the MgO-O-C-Al system into elementary tetrahedra) Gibbs energy was calculated by means of thermodynamic data (Table 1) for reactions provided in Table 2. Results of calculations are shown in Fig. 2. From data shown in Fig. 2 is it was established that in the range 1000 – 2000 K coexistence of the following phases is thermodynamically possible [20]:

1. For the system MgO-O-C in the range 1000 – 2000 K: MgO-CO_2 , MgO-CO , MgO-C (Fig. 3a).

TABLE 2. Reactions and Equations Studied for Calculating Gibbs Energy $\Delta G_T^0 = \Delta H_{298}^0 - T\Delta S_{298}^0 + \int_{298}^T \Delta C_p dT - T \int_{298}^T \Delta C_p / T dT$

Reaction	ΔG_T^0 , J/mole
(3) $2\text{Al}_2\text{O}_3 + 4\text{CO} = 3\text{CO}_2$	$357566.5713 - 4.317\ln T + 106.1766886T - 0.00265T^2 + 843000/T$
(4) $4\text{Al}_4\text{O}_4\text{C} + \text{Al} = 4\text{Al}_2\text{OC} + 3\text{Al}_3\text{O}_4$	$-46761.39476 + 18.487\ln T + 288.9177198T - 0.004805T^2 - 6860000/T$
(5) $\text{Al}_4\text{O}_4\text{C} + 4\text{Al}_2\text{O}_3 = 4\text{Al}_3\text{O}_4 + \text{C}$	$454629.8874 + 42.197\ln T - 240.9796132T - 0.010415T^2 - 9852500/T$
(6) $7\text{Al}_2\text{O}_3 + \text{Al}_4\text{O}_4\text{C} = 6\text{Al}_3\text{O}_4 + \text{CO}$	$1130336.085 + 67.857\ln T - 634.2638868T - 0.013115T^2 - 15588000/T$
(7) $3\text{Al}_2\text{O}_3 + \text{C} = 2\text{Al}_3\text{O}_4 + \text{CO}$	$675706.1978 + 25.667\ln T - 393.2842736T - 0.027T^2 - 5735500/T$
(8) $2\text{Al}_2\text{O}_3 + 3\text{C} = 2\text{CO}$	$-896773.5682 - 9.171\ln T - 545.3880211T - 0.005015T^2 + 1618500/T$
(9) $\text{Al}_2\text{O}_3 + 3\text{C} = \text{Al}_2\text{OC} + 2\text{CO}$	$803811.9588 + 9.097\ln T - 435.7785464T + 0.00411T - 1560500/T$
(10) $\text{Al}_4\text{O}_4\text{C} + 3\text{C} = 2\text{Al}_2\text{OC} + 2\text{CO}$	$710841.4094 + 9.057\ln T - 325.968159T + 0.003205T - 1502500/T$
(11) $4\text{Al}_3\text{O}_4 + 7\text{C} = 3\text{Al}_4\text{O}_4\text{C} + 4\text{CO}$	$1338935.129 - 23.937\ln T - 898.0582547T + 0.020445T^2 + 6615500/T$
(12) $\text{Al} + 3\text{Al}_4\text{O}_4\text{C} = \text{Al}_4\text{C}_3 + 3\text{Al}_3\text{O}_4$	$174615.6148 + 46.287\ln T - 72.69548544T - 0.01629T^2 - 818000/T$
(13) $\text{Al} + 12\text{Al}_2\text{OC} = 4\text{Al}_4\text{C}_3 + 3\text{Al}_3\text{O}_4$	$838748.4195 + 129.687\ln T - 1157.535101T - 0.050745T^2 - 12092000/T$
(14) $4\text{Al}_2\text{OC} = \text{Al}_4\text{O}_4\text{C} + 4\text{C}$	$221377.0096 + 27.87\ln T - 361.6132052T - 0.011485T^2 - 1308000/T$
(15) $3\text{Mg} + \text{Al}_2\text{O}_3 = 2\text{Al} + 3\text{MgO}$	$-118084.0873 + 12.587\ln T - 84.01731945T - 0.001515T - 907650/T$
(16) $2\text{MgO} + \text{C} = 2\text{Mg} + \text{CO}_2$	$816902.0712 + 13.67\ln T - 312.8700198T - 0.005365T^2 - 589400/T$
(17) $\text{MgO} + \text{C} = \text{Mg} + \text{CO}_2$	$317358.7128 + 4.567\ln T - 47.80740617T - 0.00396T + 115550/T$
(18) $\text{MgO} + \text{C} = \text{Mg} + \text{CO}$	$498320.3584 + 9.047\ln T - 265.0626137T - 0.001405T^2 + 704950/T$

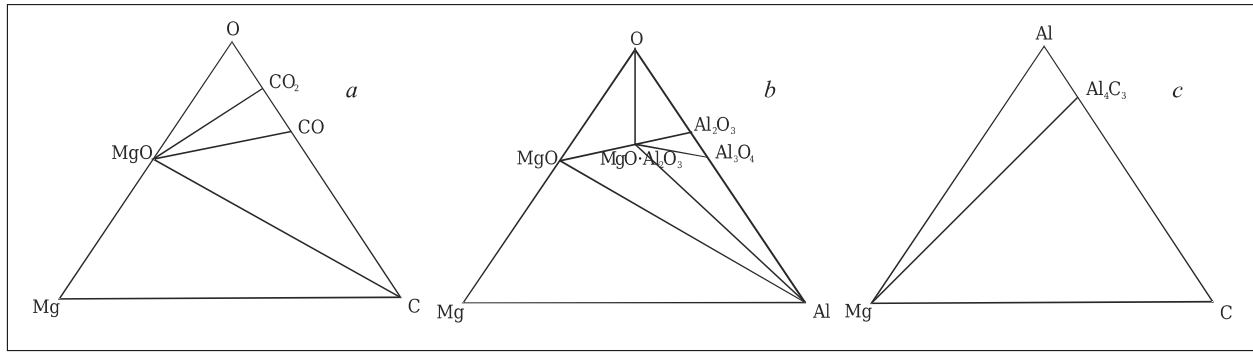


Fig. 3. Systems Mg–O–C (a), Mg–O–Al (b), and Mg–C–Al (c).

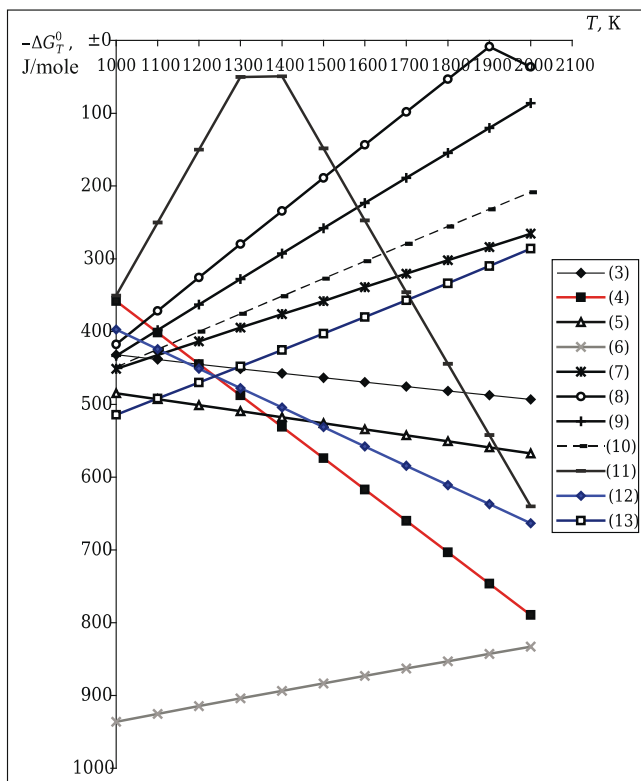


Fig. 4. Dependence of Gibbs energy ΔG_T^0 on temperature T for reactions (3) – (13) (see Table 2).

2. For the system MgO–O–Al in the range 1000 – 2000 K: MgO–Al, MgO·Al₂O₃–Al, MgO·Al₂O₃–MgO, MgO·Al₂O₃–Al₂O₃, MgO·Al₂O₃–O, MgO·Al₂O₃–Al₃O₄ (Fig. 3b).

3. For the system MgO–C–Al in the range 1000 – 2000 K: Mg–Al₄C₃ (Fig. 3c).

4. For the Al–O–C system in the range 1000 – 2000 K additional study was conducted in view of the possible conjugation of a whole series of reactions (Fig. 4) graphical dependences are shown in Fig. 4 for thermodynamically probable reactions obtained by a mirror image with respect to the temperature axis and positive values of function $\Delta G = f(T)$ of reactions considered previously (see Fig. 2).

Actually the possibility is considered of occurrence of reactions (3) – (13) (see Table 2), and in both forward and reverse directions.

The tie-line Al₂O₃–Al₄O₄C is stable over the whole range to 2000 K (see Fig. 4), the tie-line Al₂O₃–C is stable to 1005 K, and tie-line Al₄O₄C–C is stable up to 1045 K. Other reactions are less dominant for low-temperature triangulation: tie-lines Al₂OC–C and Al₂O₃–CO₂ are without alternatives from geometric topological principles. In the concentration range in the concentration ranges Al–Al₃O₄–Al₂O₃–Al₄O₄C–Al₂OC–Al₄C₃ to tie-lines are stable, Al–Al₄O₄C and Al–Al₂OC, which without variation determine subsequent triangulation of this region from geometric topological principles.

In the low temperature region of the Al–O–C system the following phase coexist (Fig. 5): Al₂O₃–CO₂, Al₂O₃–CO, Al₂O₃–C, Al₂O₃–Al₄O₄C, Al₄O₄C–Al₂OC, Al₂OC–Al₄C₃, Al₃O₄–Al₄O₄C, Al–Al₄O₄C, Al–Al₂OC, Al₄O₄C–C, and Al₂OC–C. In view of disproportionation of Al₂OC up to 1983 K [22] as a result of calculation [22] this temperature comprises 1239 K (see Fig. 4), which is explained by the sensitivity of Al₂OC decomposition temperature to the value of the original formation enthalpy for calculations. Consequently, elementary triangles with participation of Al₂OC are degenerate.

According to Figs. 4 and 5a all possible conjugations are considered, and a region of stability is established shown in the form a conjugation (imaginary or not) and ratio to triangulation. According to this calculation it has been established that in the Al–O–C system in the range 1239 – 2000 K the following phases coexist: Al₂O₃–CO₂, Al₂O₃–CO, Al₂O₃–C, Al₂O₃–Al₄O₄C, Al₄O₄C–Al₄C₃, Al₃O₄–Al₄O₄C, Al–Al₄O₄C, Al₄O₄C–C. Triangulation of this system is shown in Fig. 5b. Tetrahedral treatment of the four-component system Mg–O–C–Al in the range 1238 – 2000 K is shown in Fig. 6.

It has been confirmed that in the PC-refractory operating temperature range (1239 – 2000 K) resistant and stable compounds are composite phase of refractory MgO, C, and MgAl₂O₄, Al₄O₄C, Al₂OC, Al₃O₄, and Al₂O₃ formed, which considerably reduce carbon gasification, i.e., they protect carbon component from oxidation. Taking account of the fact

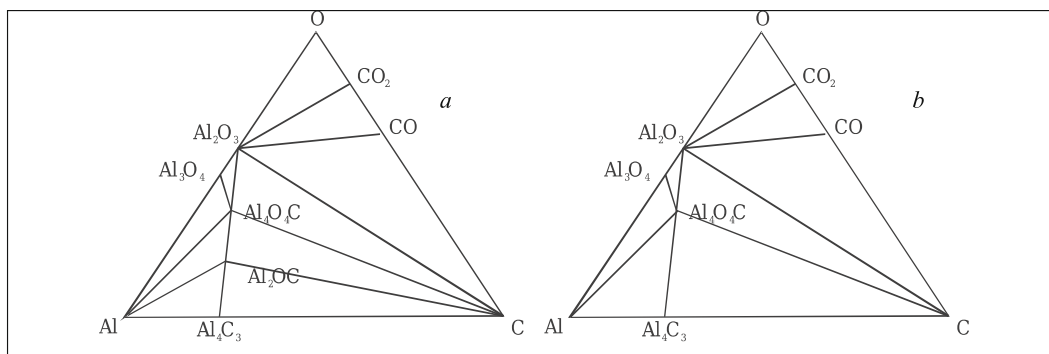


Fig. 5. Triangulation of the Al–O–C system up to 1239 K (a) and in the range 1239 – 2000 K (b).

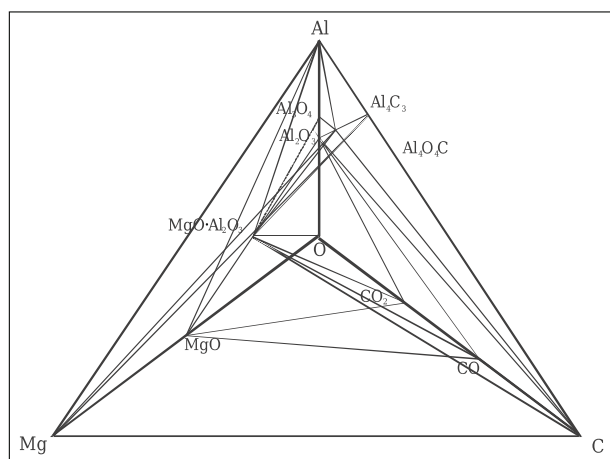
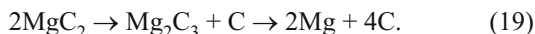


Fig. 6. Tetrahedron of the system Mg–O–C–Al in the range 1239 – 2000 K.

that operation of PC-materials proceeds in an oxidizing atmosphere and the more resistant phase according to thermodynamic calculation results is MgAl_2O_4 , with use of a small amount of Al antioxidant compositions are promising for process development located in the MgO – MgAl_2O_4 – C – CO tetrahedron. With use of antioxidant in the form of Ni powder within the composition of PC-refractory it is necessary to consider phase formation and coexistence of phases in the Mg – O – C – Ni system. A study of the composition diagram for Mg – O – C – Ni was preceded by consideration of the components of its sub-systems, and also those that include its simple and complex compositions.

In the Mg – C system there is formation of metastable carbides MgC_2 and Mg_2C_3 , that decompose by a scheme



These reactions proceed at 843 – 883 and 973 K respectively, i.e., at temperatures below the

PC-refractory service temperature. This makes it possible not to consider their thermodynamic properties in com-

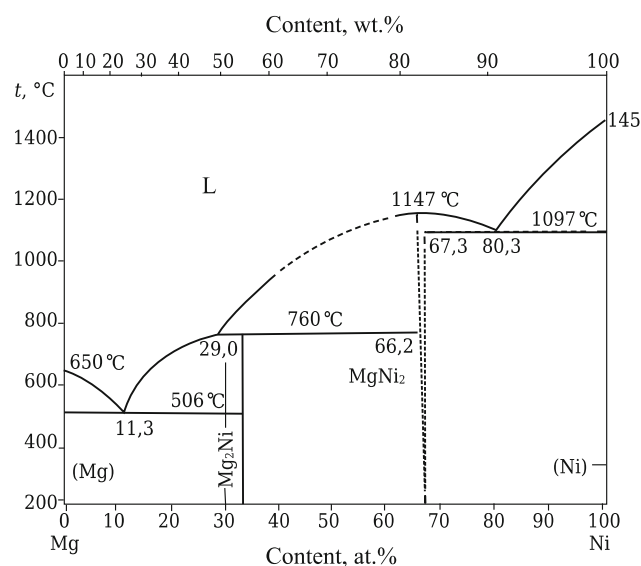


Fig. 7. Composition diagram of the Mg–Ni system [26].

posing solid phase chemical reactions with participation of magnesium carbides.

Nickel has good corrosion resistance in air, in water, in alkali, and some acids. Its melting temperature is 1728 K. At 200°C there is polymorphic transformation of α -Ni (hexagonal form) into β -Ni, which at 1073 K reacts with oxygen with formation of nickel oxide (NiO), but reaction commences from 773 K. A generalized composition diagram for Mg–Ni system is shown in Fig. 7. Valency of Mg and Ni equals 2, their ionic radii are similar, due to which metallic compounds MgNi_2 and Mg_2Ni exist. From the composition diagram for the Mg–Ni system we establish that the compound Mg_2Ni forms by a peritectic reaction at 1033 K, which is also below the PC-refractory service temperature. The compound MgNi_2 has a narrow homogeneity range and melts at 1420 K. The solubility of nickel in magnesium at 773 K reaches 0.04%. The solubility of magnesium in MgNi_2 at a temperature of about 773 K is less than 0.24%, which is shown in Fig. 7 by a dotted line separating solid solution regions.

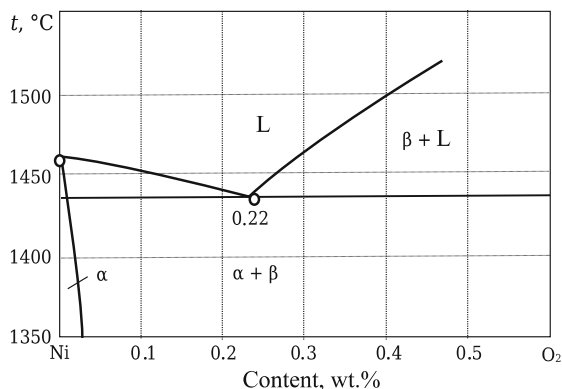


Fig. 8. Composition diagram of the Ni–O₂ system [26].

Considering the melting temperature for magnesium dinickelide it is rational to consider the effect of this compound during thermodynamic analysis of the Mg–Ni–O–C system. Corresponding composition diagrams are shown in Figs. 8 and 9 for the Ni–O₂ and Ni–C systems. As is seen from Fig. 8, nickel and oxygen have a eutectic at 1713 K. The composition of the eutectic point, determined by extrapolation of the oxygen solubility curve in molten nickel with a reduction in temperature, comprises 0.9 at.% oxygen. Reduced solubility of oxygen in nickel has been established with a reduction in temperature, which corresponds to 0.44 at.% at 1473 K and 0.073 at.% at 873 K. In this case the cubic lattice of NiO is retained to 473 K ($a = 0.4172$ nm), and below 473 K it is converted into rhombohedral ($a = 0.19518$ nm, $c = 0.7228$ nm). Thermally NiO above 1503 K becomes unstable; there is reverse dissociation [28, 29]; existence of Ni₂O₃ and Ni₃O₄ oxides is possible [29 – 31]. Possible dissociation is noted [29] to NiO₂ and Ni₂O₃ at 603 and 1143 K respectively. According to [32] Ni₃O₄ possibly exists in the form of solid solutions of NiO with Ni₂O₃. The most stable compound in the Ni–O₂ system is nickel (II) oxide [29, 32].

Carbon with nickel (see Fig. 9) forms a eutectic at $(1536 \pm 2$ K); information about the eutectic composition is varied (from 0.22 to 10% carbon). Nickel hardly dissolves in carbon, but carbon dissolves in nickel. In this case the maximum solubility of carbon in nickel reaches 2.7% at the eutectic temperature, and with a reduction in temperature carbon solubility decreases and becomes close to zero at 631 K. With a fast cooling rate (105 – 107 deg/min) and an increase in pressure it is possible to form metastable phase Ni₃C (hexagonal lattice with $a = 0.2632$ nm and $c = 0.4323$ nm). During melt cooling in similar conditions realization of eutectic Ni and Ni₃C is possible (at 1053°C, composition with 23.2 at.% carbon); at this temperature melting of metastable nickel carbide occurs at 1230 K. Increased pressure (up to 5 GPa) increases the nickel and carbon eutectic melting temperature to $(1758 \pm 5$ K), and eutectic of nickel and nickel carbide to 1570 K. In this case there is an increase in carbon solubility in nickel. It should be

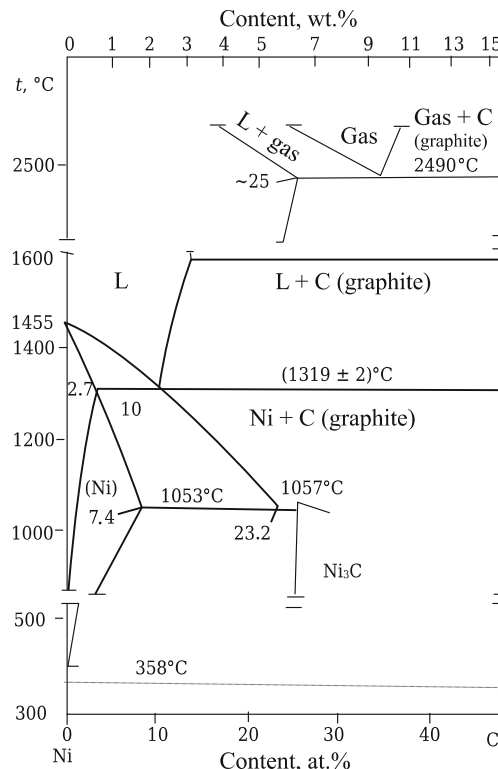
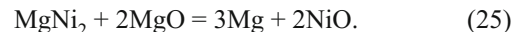
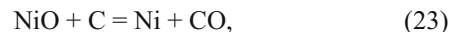
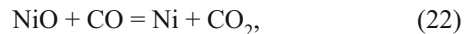


Fig. 9. Composition diagram of the Ni–C system [26].

noted that nickel carbide stability at high pressure increases, but it does not become thermodynamically stable.

In order to perform thermodynamic analysis of composition diagrams of the Mg–O–C–Ni system the following reactions were considered:



Gibbs energy equations were used in calculations without considering the temperature dependence of heat content and nickel polymorphic transformations since the temperature of these transformations is below the temperature for possible operation of refractory objects. Starting data for thermodynamic calculations are provided in Table 3. Calculation equations for the change in Gibbs energy for reaction (20) – (25) and coexistent of phases are given in Table 4.

Proceeding from the calculated Gibbs energy equations obtained it is may be concluded that there is a predominant effect of absolute value of enthalpy, and correspondingly

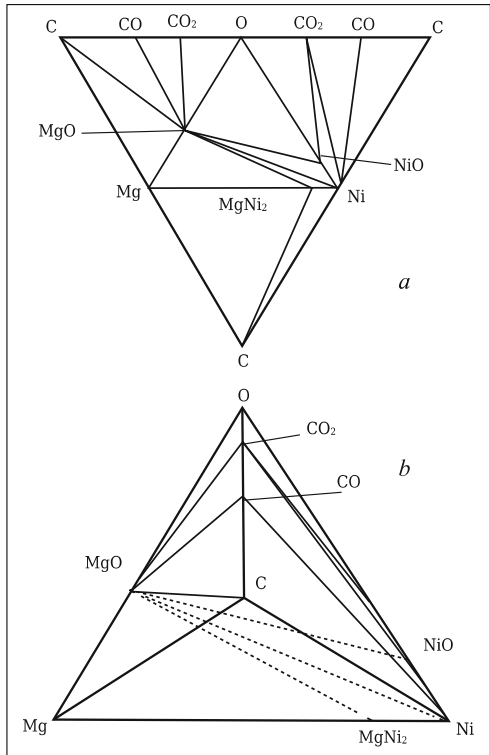
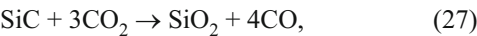


Fig. 10. Unfolded for of the structure of the composition diagram for the system Mg–C–O–Ni (a) and sub-solidus structure of this diagram (b).

clear coexistence above 1073 K of these phases (see Fig. 3a, b): MgO and CO₂, NiO and CO₂, MgO and NiO, and also MgNi₂ and C. The results obtained made it possible to accomplish triangulation of composition diagrams for the Mg–O–C–Ni system (Fig. 10). As is seen from Fig. 10a, Ni may coexist with carbon, CO, CO₂, NiO, MgO, and MgNi₂. With a reduction in the amount of Ni due to NiO formation its existence with carbon becomes impossible, i.e., reaction of nickel with oxygen commences. In view of the impossibility of controlling the amount of oxygen under PC-material

service conditions it is necessary to accomplish synthesis of compositions that are limited to phase MgO, Ni, NiO, and also Ni, MgNi₂, and MgO. In this case it will be effective to use Ni or NiO as an antioxidant, and as a precursor it is possible to use inorganic and organic nickel salts. It is well known that with respect to chemical activity nickel compounds are in this sequence [28]: NiO·Al₂O₃ → NiO·Fe₂O₃ → NiSO₄ → 2NiO·SiO₂ → NiO. Reduction of Ni ions is possible with use of chemical reducing agents sodium tetrahydaborate NaBN₄ (Ferak, FRG) and potassium hypophosphite KH₂PO₂·H₂O (Vector, RF); NaBN₄ is the strongest reducing agent, but in view of the fact that KH₂PO₂·H₂O is used together with ammonia for reduction the Ni yield in this case is higher by an order of magnitude. By changing reduction conditions it is possible to control the nickel content in specimens [29]. Also introduction of alkaline reducing agents into the PC-refractory composition is undesirable and a reducing agent nickel salt, which enters into the composition of anti-oxidant, is urotoprine, which is added to a charge of these refractories with use of PPR as a binder [7].

In order to improve the production properties of PFR and physicomechanical properties of PC-refractories based on PFR it is suggested to use [34] silicon alkoxide and its derivatives in the form of ethyl silicates and gels. As is well known [35], during conversion of these organo-silicon modifiers SiC forms as nanoparticles that strengthen carbon binder. In spite of all the advantages, SiC in oxygen-containing atmospheres is oxidized. Reaction of SiC with oxygen and gases, containing oxygen, commences above 800°C. At the surface of SiC there is formation of a protective silica film that prevents SiC from further oxidation at 1630°C. Synthesis of SiO₂ proceeds by reactions:



Therefore, considering the aforementioned transformation of PFR added during modification and graphite compo-

TABLE 3. Thermodynamic properties of Mg–C–O–Ni System Phases

Substance formula	$-\Delta H_{298}^0$, kJ/mole	ΔS_{298}^0 , J/(mole·K)	Source
MgO	601.53	27.42	[20, 31]
Mg	—	32.53	[20, 31]
CO	110.51	198.0	[20]
CO ₂	393.69	213.82	[20]
C	—	5.69	[20]
Ni	4.786	29.87	[32, 33]
NiO	6.736	37.89	[32, 33]
MgNi ₂	39.7746	88.76016	[32, 33]

TABLE 4. Formulae for Calculating Gibbs Energy of Reactions (20) – (25) and Coexisting Phases

Reaction	Calculated equation for change in Gibbs energy, J/mole	Coexistent phases
(20)	$491020 - 197.42T$	MgO and C
(21)	$318350 - 20.93T$	MgO and CO
(22)	$-281230 - 184.29T$	Ni and CO ₂
(23)	$-108560 - 184.29T$	Ni and CO
(24)	$-599580 + 13.13T$	MgO and Ni
(25)	$1229362 - 29.769T$	MgNi ₂ and MgO

nents of an organo-inorganic complex in PC-refractories during service, physicochemical processes are possible at high temperature caused by features of phase formation in the $\text{MgO} - \text{Al}_2\text{O}_3 - \text{NiO} - \text{SiO}_2$ system.⁷

There is information in publications about the structure of binary substances in the test four-component oxide system [38]. Recently information has also been accumulated about the structure of ternary sub-systems [37, 39, 40] that makes it possible to analyze the sub-solidus N–M–A–S system not studied previously. In studying the nature of the sub-solidus N–M–A–S system presence is considered within it of six binary and for ternary sub-systems including four simple oxides (N, M, A, S), six binary oxides (NA, N_2S , MA, MS, M_2S , A_3S_2), and two ternary oxides ($\text{M}_2\text{A}_2\text{S}_5$ and $\text{M}_4\text{A}_4\text{S}_2$). Thermodynamic analysis of solid phase reactions was used in the study with calculation for reference temperatures T for the change in Gibbs free energy ΔG for standard values of the change in enthalpy ΔH_{298}^0 and entropy ΔS_{298}^0 for the corresponding compounds taking account of the temperature dependence of their heat content C_p [36]. For nickel orthosilicate coefficients in the equation for the temperature dependence of heat content were calculated by the Wood and Fraser procedure [41]. Starting data for thermodynamic calculations are provided in Table 5.

The change in Gibbs energy for reaction (30) points (Table 6) to a tendency for existence of N_2S and M, which prevents the higher thermodynamic preference for coexistence of N and N_2S by reaction (29). Results of calculations for reaction (31) make it possible to triangulate the subsystem N–M–A in which presence of tie-lines N–MA and NA–MA are established. Triangulation of subsystem N–A–S [39] is

⁷ Here and subsequently abbreviations are adopted: N is NiO, M is MgO, A is Al_2O_3 , S is SiO_2 (see Table 5).

corrected by the authors of the present article in accordance with the fact that coexistence of NA with S by reaction (33) is less thermodynamically suitable than AS_2 with N_2S by reaction (44), and stable tie-lines A_3S_2 – N_2S (also at variance with coexistence of NA with S) are established from results of calculating reaction (43). In subsequent formation of tetrahedra for the N–M–A–S system these situations were not considered by the authors. Analysis of results of calculations for the reverse reaction (38) points to apparent evidence of coexistence of N and $\text{M}_2\text{A}_2\text{S}_5$ up to about 1097 K, but this contradicts the greater thermodynamic probability of reaction of these phases by reaction (40), for which stability of N_2S –MA tie-lines is determined. Stability of the three-phase composite NA, MS, S by reaction (39) is not confirmed since coexistence of MA with N_2S is more thermodynamically probable (reaction (46), see Table 6). Results of calculating the rest of the reactions of Table 6 is simple for analysis (including with triangulation of the N–M–S subsystem), and in clear form points to the direction of occurrence of coexisting processes that made it possible to establish [42] stable tie-lines for subsequent tetrahedral formation for the N–M–A–S system.

Nickel orthosilicate (N_2S) during its synthesis in PC-refractory and reacting phases coexists with all phases in the test N–M–A–S system above 1287 K, but at lower temperature it only reacts with M. Correspondingly, N_2S is present in elementary tetrahedral with the maximum total volume and has the greatest probability of existence, which points to good stability of N_2S in the test system. The high probability of existence is also noted in [42] for MA, M_2S , and M in the region up to 1287 K. At higher temperature the situation changes and alongside N_2S the is high probability of existence of a solid solution (M_4A_5) M, and cordierite solid solution ($\text{M}_4\text{A}_5\text{S}_{10}$). The lowest probability for existence is noted for NA, A_3S_2 , and A in the whole temperature range. In the

TABLE 5. Thermodynamic Data for Compounds of the M–A–S–N System

Designation (compound)	$-\Delta H_{298}^0$, kJ/mole	Source	S_{298}^0 , J/(mole·K)	Source	$C_p = a + b \times 10^{-3} T - c \cdot 10^5 T^{-2}$, J/(mole·K)			
					<i>a</i>	<i>b</i>	<i>c</i>	Source
A (corundum)	1676.0577	[2]	50.92	[7]	115.02	11.8	35.06	[35]
S (α -quartz)	910.4383	[10]	41.46344	[10]	43.89016	1.00416	6.02496	[34]
MA (spinel)	2300.7816	[8]	80.58384	[10]	153.9712	26.7776	40.91952	[34]
MS (clinoenstatite)	1548.9	[7]	67.86	[7]	102.7172	19.83216	26.27552	[36]
M_2S (forsterite)	2171.9144	[8]	95.14	[7]	149.83	27.36	35.65	[35]
A_3S_2 (mullite)	6816.9912	[9]	269.57512	[9]	454.29872	66.1072	125.3108	[21]
$\text{M}_2\text{A}_2\text{S}_5$ (cordierite)	9158.3576	[8]	407.1032	[9]	601.78472	107.9472	161.5024	[21]
$\text{M}_4\text{A}_4\text{S}_2$ (sapphirine)	11107.497	[2]	390.34172	[2]	654.23205	117.35512	175.57781	[37]
N (NiO)	239.74	[7]	37.99	[7]	46.78	8.46	0	[35]
NA (aluminum-nickel spinel)	1915.4	[7]	92.5	[7]	159.2012	23.34672	30.7524	[34]
N_2S (nickel orthosilicate)	1429.7	[7]	111.3	[7]	119.589	20.935	0	—
M (MgO)	601.7	[7]	26.94	[7]	48.982	3.138	11.439	[35]

low temperature region the maximum volume is occupied by elementary tetrahedral N–M–MA–M₂S, represented by a four-phase combination of refractory compounds.

Second, with respect to occupied volume there is also an elementary tetrahedron with refractory compounds at its tips N–M–MA–M₂S. In spite of the fact that the volume of elementary tetrahedron N–M–MA–M₂S is at a maximum and the degree of its asymmetry is low (i.e., there are apparent prerequisites for exclusion of high precision of dispensing original components during synthesis of materials with their predicted phase composition in a concentration region of this tetrahedron), it is necessary to consider the possibility of chemical reaction of NiO with M₂S [42, and correspondingly unfavorable structural changes. Taking account of the Ni content in complex antioxidant in an amount of 0.25 – 0.75% (and SiC, which may oxidize to SiO₂, only in an amount of fractions of a percentage). This reaction is almost impossible. In the high temperature region the maximum volume in the system is occupied by the aforementioned elementary tetrahedron that are represented by refractory phases and have comparatively low asymmetry.

The characteristics established for the sub-solidus structure of the N–M–A–S system (Fig. 11) make it possible to predict the phase composition of PC-materials within whose composition complex antioxidant Al + SiC + Ni(NiO) is used, a precursor of three successive compounds that are modifications of PPR and graphite. Considering the fact that complex antioxidant is introduced into PC-specimen composition in an amount of not more than 2%, during service above 1287 K coexisting phases will be M, MA, N, and also

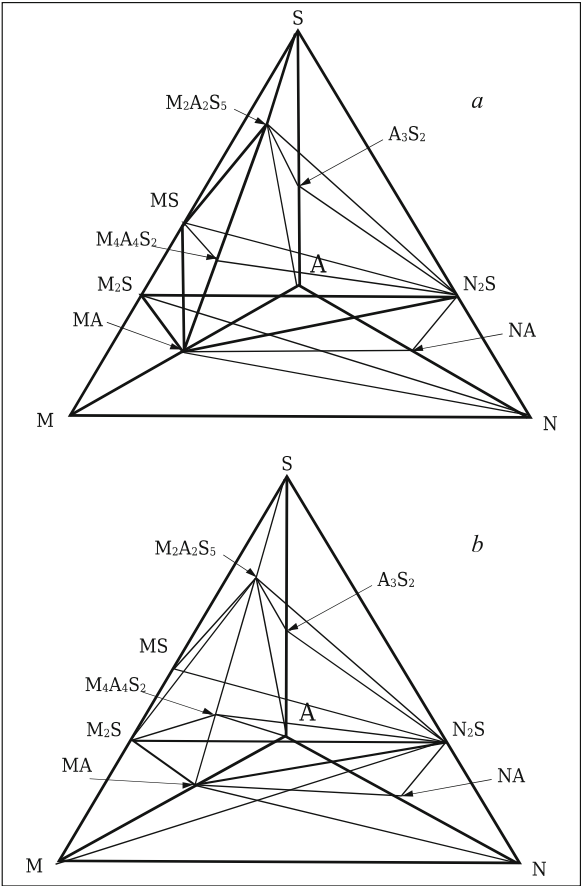


Fig. 11. Sub-solidus structure of the M–A–S–N system up to 1287 K (a) and above 1287 K (b).

TABLE 6. Thermodynamic Calculation Results

Reaction	Change in Gibbs energy, kJ/mole, at temperature, K				
	800	1000	1200	1300	1500
(29) 22N + M ₂ S = N ₂ S + 2M	15.723	10.436	3.476	–0.580	–9.771
(30) 2N + MS = N ₂ S + M	–5.483	–10.515	–17.110	–20.943	–29.590
(31) N + MA = M + NA	23.540	24.530	25.024	24.131	24.191
(32) 4N + A ₃ S ₂ = 3A + 2N ₂ S	–90.427	–94.520	–101.739	–106.406	–117.684
(33) 3N + A ₃ S ₂ = 3NA + 2S	–19.518	–21.586	–25.522	–28.116	–34.588
(34) 7N + A ₃ S ₂ = 3NA + 2N ₂ S	–96.639	–102.199	–110.773	–116.068	–128.483
(35) 4N + M ₄ A ₄ S ₂ = 4NA + 2M ₂ S	70.309	85.446	104.211	114.755	137.873
(36) 4N + M ₄ A ₄ S ₂ + 2S = 4NA + 4MS	46.565	67.767	94.353	109.430	142.790
(37) 4N + M ₄ A ₄ S ₂ = 2N ₂ S + 4MA	7.598	11.018	14.9518	17.074	21.575
(38) 2N + M ₂ A ₂ S ₅ = 2NA + 2MS + 4S	9.440	3.880	–5.460	–11.458	–25.969
(39) 2N + M ₂ A ₂ S ₅ = 2NA + 2MS + 3S	–2.432	–4.959	–10.388	–14.121	–23.511
(40) 10N + M ₂ A ₂ S ₅ = 5N ₂ S + 2MA	–176.117	–194.559	–220.592	–236.159	–271.909
(41) 16N + 2M ₂ A ₂ S ₅ = 8N ₂ S + M ₄ A ₄ S ₂	–359.914	–400.135	–456.136	–489.390	–565.392
(42) 2N ₂ S + M ₄ A ₄ S ₂ = 4NA + 4MS	123.686	148.379	179.606	197.360	236.684
(43) A ₃ S ₂ + 4NA = 7A + 2N ₂ S	–82.145	–84.282	–89.692	–93.523	–103.287
(44) 2A ₃ S ₂ + 3NpS = 6NA + 7S	76.646	77.747	76.828	75.616	71.666
(45) 2N + 2MS = M ₂ S + N ₂ S	–26.758	–31.576	–37.848	–41.474	–49.620
(46) 2NA + M ₂ S = 2MA + N ₂ S	–31.356	–37.214	–41.630	–48.826	–58.149

N_2S (in the case of synthesis with a very low content of modifying addition of PPR in the form of tetraoxysilane).

CONCLUSION

With introduction of an organo-inorganic complex, including silicon alkoxide and inorganic or organic nickel salts, into the composition of PC-refractory with antioxidant (Al) used normally, complex antioxidant Al + SiC + Ni(NiO) is created whose components coexist with periclase and carbon and may be used in order to protect PC-refractory from oxidation. In other words, PFR and graphite added as modifiers together with Al additive will first converted to SiC and Ni, which oxidize themselves, restraining graphite from oxidation, being converted into SiO_2 and NiO oxides. In the four-components N–M–A–S system formed periclase coexists with spinel and nickel oxide to 1287 K and above 1287 K with N_2S . However, considering the predominant amount of spinel formed over the very small amount of N_2S phase possibly synthesized (which may coexist with 11 phases in the system), during PC-refractory service with complex antioxidant an improvement will be observed in physicomechanical properties and increased resistance to metal and slag due to spinel synthesis.

REFERENCES

1. S. Okke, S. Andre, Zh-P. Érauv, et al., "Characteristics of oxidation processes in carbon-containing refractory materials in metallurgy," *Ogneupory. Tekhn. Keram.* No. 1, 55 – 60 (2008).
2. E. V. Krovokorytov, A. G. Gur'ev, and B. I. POLyak, "High carbon binders in refractory object technology and ceramic corrosion resistance," *Steklo. Keram.*, No. 5, 12 – 15 (1998).
3. W. Slusser, USA Patent 5438026, MPK7 C 04 B 35/01, C 04 B 35/66. Magnesite-carbon refractories and shapes made there from with improved thermal stress tolerance. Claimant and patent holder Indresco, Inc., No. 19910232381, Claim 04.25.91, Publ. 08.01.95.
4. C. Taffin and J. Poirier, "The behavior of the metal additives in Mg- and Al_2O_3 -C refractories," *Interceram.*, **43**(5), 458 – 460 (1994).
5. S. K. Sadrnezhaad, Z. A. Nemat, S. Mahshid, et al., "Effect of Al antioxidant on the rate of oxidation of carbon in Mg- refractory," *J. Am. Ceram. Soc.*, **90**(2), 509 – 515 (2007).
6. G. D. Semchenko, L. A. Angolenko, V. V. Povshuk, and A. S. Katiukha, *Unmolded Refractory Composition Al_2O_3 -SiC-C* (G. D. Semchenko, editor) [in Russian], Graf-OKS, Khar'kov (2015).
7. I. D. Kashcheev, *Oxide-Carbon Refractories* [in Russian], Internet Inzhiniring, Moscow (2000).
8. V. G. Bbamburov, O. V. Sintseva, V. P. Semyannikov, et al., "Antioxidants in carbon-containing refractories," *Ogneupory Tekhn. Keram.*, No. 2, 2 – 5 (2000).
9. V. G. Bbamburov and O. V. Sivtsova, "Antioxidizing agents in carbon-containing refractories," *Khim. Tverd. Tel., Strukt. Prim. Novykh. Neorgan. Mater.*, No. 2, 66 – 72 (1998).
10. Peter Barhta and Helge Jasnsen, German Patent 19954893, MPK7 C 04 B 35/66. Carbon-containing refractory with improved oxidation resistance and its preparation method Claimant and patent holder Refractech Holding, GmbH & Co. KG. No. 19954893, Claim 11.15.99, Publ. 05.17.05.
11. S. K. Sadrnezhaad, S. Mahshid, B. Hashemi, et al., "Oxidation mechanism of C in MgO–C refractory bricks," *J. Europ. Ceram. Soc.*, **89**(4), 1308 – 1316 (2006).
12. I. D. Kashcheev and L. V. Serova, "Interaction between aluminum and periclase-carbon components," *Refract. Indust. Ceram.*, **47**(2), 125 – 127 (2006).
13. I. G. Ochagova, "Periclase-carbon refractories for lining oxygen converters, arc furnaces and steel extra-furnace treatment units," *Nov. Chern. Met. Rubezh.*, No. 1, 137 – 149 (1995).
14. S. Hiroyuki, K. Yukinobu, "Trends of refractories for BOF," Shinagawa Technical Report **40**, 51 – 62 (1997).
15. K. Tada, O. Nomura, and H. Nisio, "Effect of aluminum on compaction of magnesia-carbon refractory object structures," *Taikabutsu*, **2**(2), 6065 (1999).
16. M. S. Khrushchev, "Thermodynamic study of the Al–O–C system at high temperature," *Izv. Akad. Nauk SSSR, Metall.*, No. 6, 46 – 49 (1969).
17. N. E. Filinenko, I. V. Lavrov, and S. V. Andreev, "Aluminum oxycarbides," *DAN SSSR*, **125**(1), 155 – 158 (1959).
18. A. G. Vodp'yanov, A. V. Serebyrakova, and G. M. Kozhenikova, "Kinetics and mechanism of reaction of aluminum oxide with carbon," *Zv. Akad. Nauk SSSR, Metall.*, No. 1, 43 – 47 (1982).
19. I. S. Kulikov, *Thermodynamics of carbides and Nitrides: Handbook* [in Russian], Metallurgiya, Moscow 91988).
20. O. M. Borisenko, G. D. Semchenko, and D. A. Brazhnik, "Thermodynamic evaluation of phase formation in the MgO–C–Al system," Contemporary problem of thermodynamics and thermophysics: All-Russia Conf. devoted to 110 years from birth of Corr. Mem. AN SSSR P. G. Strelkov, 1 – 3 December (2009), INKh SO RAN, Novosibirsk (2009).
21. A. S. Berezhnoi, *Multicomponent Oxide Systems* [in Russian], Naukova Dumka, Kiev (1970).
22. V. L. Klimov, G. A. Bergman, and O. K. Karlina, "Thermodynamic properties of aluminum oxides: conformity with Al_2O_3 – Al_4C_3 composition diagram," http://thermophysics.ru/pdf_doc/Klimov_dr.doc.
23. R. A. Lidin, V. A. Molochko, and L. L. Andreeva, *Chemical Properties of Inorganic Substances* [in Russian], Khimiya, Moscow (2000).
24. R. Ripan and I. Chetyanu, *Inorganic Chemistry in 2 Vol., Vol. 2, Metal Chemistry* [in Russian], Mir, Moscow (1972).
25. Ya. A. Ugai, *Inorganic Chemistry* [in Russian], Vysshaya Shkola, Moscow (1989).
26. I. S. Kulikov, *Oxide Thermodynamics* [in Russian], Metallurgiya, Moscow (1986).
27. Yu. Tret'yakov, *Nonstoichiometric Oxide Chemistry* [in Russian], MGU, Moscow (1974).
28. V. S. Chekushkin, and N. V. Oleinikova, "Thermodynamic reduction of nickel and cobalt from oxide-sulfate compounds," *J. Sib. Fed. Univ. Eng. Technol.*, No. 1, 58 – 67 (2008).
29. A. M. Mikhailidi, N. E. Kotel'nikova, and M. P. Novasiv, "Preparation of nickel particles in a matrix of hydrocellulose nickel activated by alkali solutions," *Khim. Rastit. Syr.*, No. 3, 21 – 28 (2010).
30. G. D. Semchenko, V. V. Povshuk, D. A. Brazhnik, et al., "Creation of a combined liquid phenolfomaldehyde antioxidant-modifier for improving periclase-carbon refractory life," *Refract. Indust. Ceram.*, **56**(6), 644 – 647 (2016).
31. V. A. Ryabin, M. A. Ostroumov, and T. F. Smit, *Thermodynamic Properties of Substances* [in Russian], Khimiya, Leningrad (1972).

32. A. A. Pashchenko, *Cement theory* [in Russian], Budivel'nik., Kiev (1991).
33. M. T. Mel'nik and N. N. Shapovalova, "Refractory concrete based on alumina cement with addition active alumina," *Ogneupor*, No. 10, 56 – 57 (1974).
34. O. Kubashevsky and S. B. Alcock, *Metallurgical Thermodynamics* [Russian translation], Metallurgiya, Moscow (1982).
35. Yu. D. Tret'yakov, *Solid Phase Reactions* [in Russian], Khimiya, Moscow (1978).
36. V. I. Babushkin, G. M. Matveev, and O. P. Mchedlov-Petrosyan, *Silicate Thermodynamics* [in Russian], Stroiizdat, Moscow (1986).
37. N. A. Toropov, V. I. Barzakovskii, V. V. Lapin, et al., *Silicate System Composition Diagrams: handbook, Ternary Systems* [in Russian], Nauka, Leningrad Sect, Leningrad (1972).
38. N. A. Toropov, V. I. Barzakovskii, V. V. Lapin, and N. N. Kurtsseva, *Silicate System Composition Diagrams: handbook, Binary Systems* [in Russian], Nauka, Leningrad Sect, Leningrad (1972).
39. B. Phillips, J. J. Hutta, and I. Warshaw, "Phase equilibria in the system $\text{NiO-Al}_2\text{O}_3\text{-SiO}_2$," *J. Am. Ceram. Soc.*, **46**(12), 579 – 583 (1963).
40. S. M. Loginov, G. D. Semchenko, D. A. Kobyzeva, and V. I. Babushkin, "Thermodynamics of phase interactions in sub-solidus of system $\text{MgO-Al}_2\text{O}_3\text{-SiO}_2$," *Ogneupor. Tekhn. Keram.*, No. 12, 9 – 15 (2001).
41. B. Wood and D. Fraser, *Bases of Thermodynamics for Geologists* [Russian translation], Mir, Moscow (1981).
42. D. A. Kobyzeva, S. M. Logvinkov, G. D. Semchenko, and D. S. Logvinkov, "Thermodynamic aspects of phase formation for composites of the system $\text{MgO-Al}_2\text{O}_3\text{-SiO}_2\text{-NiO}$," *Shukov BGU Vestnik, Proc. Internat. Congr. Contemporary technology in building material and construction industry*, No. 5, 139 – 141 (2003).